



Periodicity and frequency coding in human auditory cortex

Journal:	<i>European Journal of Neuroscience</i>
Manuscript ID:	EJN-2006-07-11068.R1
Manuscript Type:	Research Report
Date Submitted by the Author:	n/a
Complete List of Authors:	Hall, Deborah; MRC, Institute of Hearing Research Edmondson-Jones, Andrew; MRC, Institute of Hearing Research Fridriksson, Julius; University of South Carolina, Department of Communication Sciences and Disorders
Key Words:	Auditory cortex, pitch, neuroimaging, humans



view

Receiving editor : N. Logothetis (G. Rainer)

Periodicity and frequency coding in human auditory cortex
EJN-2006-07-11068 : revised manuscript

Deborah A. Hall^{1*}, A. Mark Edmondson-Jones¹ and Julius Fridriksson²

¹ MRC Institute of Hearing Research,
University Park,
Nottingham,
NG7 2RD,
UK.

² Dept. of Communication Sciences and Disorders,
University of South Carolina,
Columbia,
SC 29208,
USA.

Contact information :

* Deborah Hall is the corresponding author
email : d.hall@ihr.mrc.ac.uk
Tel : +44 (115) 922 3431
Fax : +44 (115) 951 8503

Running title : Periodicity and frequency coding in human auditory cortex

Total number of pages	24
Word count in whole manuscript	5,47 (inc. refs and legends)
Word count in Abstract	187
Word count in Introduction	490
Total number of figures	3
Total number of tables	3
Total number of equations	0
Keywords	neuroimaging; auditory cortex; pitch; humans.

Abstract

Understanding the neural coding of pitch and frequency is fundamental to the understanding of speech comprehension, music perception and the segregation of concurrent sound sources. Neuroimaging has made important contributions to defining the pattern of frequency-sensitivity in humans. However, the precise way in which pitch sensitivity relates to these frequency-dependent regions remains unclear. Single-frequency tones also cannot be used to test this hypothesis since their pitch always equals their frequency. Here, temporal pitch (periodicity) and frequency coding were dissociated using stimuli that were bandpassed in different frequency spectra (centre frequencies 800 and 4500 Hz), yet were matched in their pitch characteristics. Cortical responses to both pitch-evoking stimuli typically occurred within a region that was also responsive to low frequencies. Its location extended across both primary and nonprimary auditory cortex. An additional control experiment demonstrated that this pitch-related effect was not simply caused by the generation of combination tones. Our findings support recent neurophysiological evidence for a cortical representation of pitch at the lateral border of the primary auditory cortex, while revealing new evidence that additional auditory fields are also likely to play a role in pitch coding.

Introduction

Frequency is a well-established general organising principle throughout the mammalian auditory system and tonotopicity (the ordered spatial mapping of frequency sensitivity across auditory cortical fields) is organised in a consistent pattern across individuals. The sensation of pitch is associated with regularly repeating waveforms and pitch can be calculated from either the relative separation of the spectral components (along the frequency axis) or the periodicity (along the time axis) of a complex sound. It has correspondingly been suggested that pitch can be extracted centrally either in the frequency domain (spectral analysis) or in the time domain (period analysis). At least one study searching for the neural basis of pitch has found no selectivity in the primary auditory cortex for any stimulus parameters that might be relevant for pitch perception (Schwartz and Tomlinson, 1990). In contrast, other electrophysiological data have suggested that response sensitivity to periodicity is laid out in a spatially systematic manner, at least within the gerbil's primary auditory cortex (Schulze and Langner, 1997; Schulze et al., 2002). Specifically, the spatial tuning for high-envelope frequencies, which generate a periodicity pitch, forms a circular periodicity gradient that is superimposed onto the linear tonotopic gradient. The precise geometry of the periodotopic gradient and its relationship with the tonotopic gradient varied across animals. Nevertheless these authors report that the pitch-sensitive region typically encompasses a low-frequency portion of the primary auditory cortex. Although the current status of the periodicity gradient is unclear, Bendor and Wang (2005) have recently confirmed an overlapping representation of pitch and frequency in marmosets with pitch-sensitive neurons biased towards lower frequency-sensitive regions at the anterolateral border of the primary auditory cortex. These neurons were responsive not only to low frequency pure tones, but also a range of pitch-evoking stimuli including missing fundamental harmonic complex sounds, click trains and iterated-ripple-noise (IRN) which can each generate a virtual pitch without energy at the fundamental frequency.

At present, the relationship between the representations of pitch and frequency in humans can only be inferred from a synthesis of experiments which have examined these attributes separately and in different listeners. Given the known variability in auditory functional anatomy across different listeners (Patterson et al., 2002; Talavage et al., 2000; 2004), it is important to validate the case in humans. We address this by testing two specific predictions; i) pitch and frequency representations are co-localised in the human auditory cortex, and ii) the common region of activation is located within a low-frequency dependent region that encompasses the anterolateral border of the primary auditory cortex. To co-localise the cortical region that is sensitive to pitch and frequency, our design crossed frequency (bandpassed at low and high centre frequencies) with stimulus type (single-frequency tone, IRN and random noise) to generate six stimulus conditions that each excited an equivalent distance along the simulated tonotopic scale (Figure 1). IRN was used to generate pitch in the time domain, so that period analysis could be isolated from that of spectral analysis.

** Figure 1 **

Experiment 1 : Materials and methods

Subjects

Fourteen listeners volunteered to take part (mean age 31 years, range 20-48, five male, 12 right-handed). Subjects all had a hearing level ≤ 20 dB HL between 0.5 and 8 kHz and had no history of neurological disorders. All subjects gave informed written consent to participate. The study was approved by the Medical School Research Ethics Committee, University of Nottingham and conforms with the code of ethics of the World Medical Association.

Stimuli

The stimuli were sequences of pure tones, random noise bursts and iterated-ripple-noise (IRN) bursts. IRN is perceived as a pitch superimposed on a background hiss. Each of the three types of carrier sound was presented at a low (800 Hz) and high (4500 Hz) centre frequency. Both the noise and IRN bursts had a 0.75 octave bandwidth around each centre frequency, hence the low-frequency noise contained frequencies between 617 and 1038 Hz and the high-frequency noise between 3470 and 5836 Hz. For any IRN, pitch comes from having a periodic temporal structure that is created by delaying and adding the noise back onto itself (Yost et al., 1996). Increasing the number of delay-and-add iterations increases the temporal regularity in the signal, and hence the salience of the pitch. In the present experiment, all IRN bursts had a delay of 16.67 ms **and a gain of +1.0**, giving a pitch of 60 Hz. Repeating this delay-and-add process 16 times generated an IRN with a highly salient pitch percept. Temporal models of pitch perception predict that when the delay of both low- and high-spectrum IRN is the same then they have the same pitch.

The centre frequencies and passbands were selected to meet two criteria. First, conditions that differed in centre frequency should generate separately resolvable activation patterns across the auditory cortex given the spatial resolution of the functional magnetic resonance imaging (fMRI) protocol. Based on previous data, two pure tones separated in frequency by two octaves frequency are expected to elicit activation peaks approximately 6 mm apart along the tonotopic gradient (Romani et al., 1982; Pantev et al., 1988). Given that our selected centre frequencies were separated by five octaves and our resolution was 3.25 mm³, the activation peaks should be easily resolvable. Second, conditions matched for centre frequency should evoke similar neural excitation patterns across the basilar membrane. Both the noise and IRN were matched for spectral energy at each of the two centre frequencies. The IRN and the noise excited the same frequency channels of neural activity, according to a computational model of cochlear function (Patterson et al., 1996), and simulations of the neural excitation pattern shown in Figure 1 demonstrate them to be equivalent. Following the **neuroimaging** studies of Griffiths et al. (1998) and Patterson et al. (2002), the low-frequency cut offs were chosen to ensure that neither IRN stimulus contained energy at the frequency of the 60 Hz pitch nor contained any resolved spectral peaks at the higher frequencies.

Hence, the pitch percept is wholly based on extracting time intervals (periodicity) rather than spectral peaks from the neural pattern in the auditory nerve.

Each sound condition was made up of a sequence of 16 bursts that were 475 ms in duration with 50-ms linear onset and offset ramps and separated by 25-ms gaps of silence. **These parameters were chosen because a presentation rate of 2 Hz elicits sustained auditory cortical activation with a minimal, but nevertheless clearly perceptible, gaps between bursts (Harms and Melcher, 2002).** The sounds were sampled at 44100 Hz and sound energy was constant across all stimulus types.

fMRI protocol and listening task

The scanning study consisted of one 30-minute listening experiment, plus an 8-minute anatomical scan. In the experiment, subjects lay with their eyes closed while listening to sound stimuli presented using an integrated functional imaging system (MRI Devices Corporation, USA). The sound output level was fixed for all subjects and the average output, measured at the headphones using a sound level meter, was 86 dB SPL so that the stimuli were clearly audible with respect to the scanner noise. Sound sequences were presented in a randomised order interleaved with a silent condition to provide a baseline control. Each sound condition was presented 28 times to provide reliable estimates of stimulus-specific activation. A simple task to confirm subjects' arousal was to make a right index finger button press at each occurrence of a silent condition. All subjects complied with the task instructions, but accuracy was not logged.

Scanning was performed on a Philips 3 T MRI Intera using an 8-channel SENSE head coil with a Velcro strap to gently restrain head movements. An anatomical scan provided a 1 mm³ resolution image of the brain and covered a 256 x 256 matrix in 160 sagittal slices. Functional scans (64 x 64 matrix, TE = 30 ms) consisted of 32 slices taken in an oblique-axial plane with a voxel size of 3.25 mm³. Functional scanning used a SENSE factor of 2 to reduce image distortions. In total, 196 functional scans were collected at regular 9 s intervals. Each scan had an acquisition time of

1.647 s, enabling the stimulus sequence to be presented in the quiet periods between scans. This protocol has been shown to avoid any interference of the scanner acoustic noise (Hall et al., 1999).

Data analysis

Analysis was conducted using SPM2 (<http://www.fil.ion.ucl.ac.uk/spm>). The functional time series was realigned to the middle scan of the series and the anatomical scan was then coregistered to the mean of the realigned images so that, for each individual, both types of scan mapped onto one another. Individual datasets were normalized to a standard brain space by first calculating the linear and nonlinear transformations required to map the segmented grey matter of the anatomical scan to a grey matter T1-template. These transformations were subsequently applied to the coregistered anatomical and functional scans to maintain a reasonably precise mapping between structure and function. The functional data were upsampled to 2 mm³ resolution and then smoothed with a Gaussian filter of 5 mm³ (full width half maximum) to reduce the effects of residual population variability in normalised brain shape.

A general linear model was first fit to each individual's data. The model described the time series signal at each voxel as a linear combination of the six stimulus conditions and the six head movement parameters, plus the mean and a residual error term. Statistical contrasts defining each of the differential responses to frequency and periodicity were specified by a *T* contrast between the relevant stimulus conditions. For example, low-frequency activation was identified by subtracting the high-frequency pure tone and noise conditions from the twomatched low -frequency conditions, while high-frequency activation was identified by the converse statistical comparison. The response to periodicity was represented by subtracting the two noise conditions from the two IRNs. Second-level, one-sample T tests were performed on the resulting statistic images to account for both the within- and between-subjects variance across the group and thus enable an estimate of the generality of each effect.

Results

Joint sensitivity to periodicity and frequency

** Table 1 **

To test the first prediction, the dominant patterns of periodicity and frequency sensitivity were determined using one-sample T tests. We used two different probability thresholds i) $p < 0.001$ uncorrected and, ii) $p < 0.05$ with control for a false-discovery rate, to explore the patterns of activation within a region of interest (ROI) defined by the outermost boundary of the sum of the three primary auditory fields (Te1.0, Te1.1 and Te1.2) on Heschl's gyrus (HG) (Morosan et al., 2001) and the planum temporale (PT) (Westbury et al., 1999). The location and extent of significant activity are reported in Table 1. We define low-frequency-dependent response regions (low-FDRRs) as those exhibiting a significantly greater response to the tones and noise with a low centre frequency than a high centre frequency. For the general frequency contrast that combined both tone and noise conditions, low-FDRRs (Figure 2A, blue) encompassed both left and right auditory cortices and were largely centred at the lateral endpoints of HG and behind, in an anterolateral portion of PT. High-frequency dependent response regions (high-FDRRs) reached only an uncorrected level of significance on the right side (Figure 2A, red). Generally, high-FDRRs occupied sites medial to the low-FDRRs. Periodicity-related activation partly engaged the posterior part of HG in both hemispheres, but the peaks were predominantly located behind, in adjacent portions of PT. In Figure 2A, the response to periodicity is marked in green and yellow, where the latter highlights activity that co-occurred with one of the frequency regions. In fact, 44% of the periodicity response occurred within voxels that also responded to low frequencies (23/77 voxels on the left side and 108/220 on the right). The response to temporal pitch did *not* overlap with the high-FDRR. As Figure 2A clearly demonstrates, the general low-FDRR was by far the most extensive region of activity and the effect of temporal pitch partly overlapped with it in a restricted area that was centred on lateral HG and anterolateral PT. Although Figure 2 illustrates only those results

using the uncorrected statistical threshold ($p < 0.001$), a very similar pattern was observed using the corrected threshold ($p < 0.05$).

**** Figure 2 ****

The study design enabled us to further explore the typical pattern of responses to periodicity and frequency in more detail. The following two sections describe these additional analyses.

Does the conjoint response to periodicity and low frequency involve the primary auditory area ?

Our first concern was how well the region co-sensitive to temporal pitch and low frequency might correspond to primary auditory cortex. It is well-documented that single frequency tones strongly drive neurons in primary auditory fields, whereas they weakly drive neurons in nonprimary auditory cortex. Hence, a strong response to pure tones can serve as a marker for the primary auditory cortex (Wessinger et al., 2001). To derive our functional marker for the low-frequency portion of the primary auditory area, we therefore computed the low-FDRR for the pure tone and noise contrasts separately ($p < 0.001$ uncorrected). As expected, the frequency-related activation was more extensive for the noise than for the tone contrast (821 vs 616 activated voxels) (Figure 2B-C). For the pure tones, the co-localisation of low frequency and periodicity appeared to be somewhat restricted to portions of HG (see the right hemisphere of slice 2 of Figure 2B). We quantified this degree of coincidence between the conjoint activity (for periodicity and the tone-alone low-FDRR) and the primary auditory cortex. The latter region was anatomically defined using probabilistic estimates of Te1.0, Te1.1 and Te1.2 given by the SPM2 anatomy toolbox (Eickhoff et al., 2005; Morosan et al., 2001). In the right hemisphere, 60% (29/48 voxels) of the conjoint activity involved these primary fields, while in the left hemisphere it was 47% (8.4/18 voxels). The peaks of the conjoint activity were located in lateral HG (Te1.2) with a probability of 70% in the right (x 58, y -6, z 0) and 10% in the left (x -54, y -18, z 6). Thus, as far as it is possible to determine from the

functional and anatomical evidence, the region jointly sensitive to periodicity and low frequency probably includes the primary auditory cortex, although not exclusively.

A consistent mapping of periodicity? One conceptualisation of a pitch map is that pitch values are represented in a spatially-ordered manner and that the response to individual values of pitch is invariant across different stimulus types. For example, preliminary neurophysiological demonstrations have revealed that pitch-selective neurons share a similar tuning for pure tones and missing fundamental harmonic-complex tones (Bendor and Wang, 2005). Thus, pitch constancy would predict that stimuli with an identical periodicity but different spectra will still share a neural code for pitch. The data permit us to examine this issue by considering the effects of periodicity separately for the two IRN conditions. We define the effect of low-spectrum IRN by the subtraction of the low-frequency noise from the low-frequency IRN. The effect of the high-spectrum IRN is the equivalent contrast for the high-frequency stimuli. Since the two pairs of comparisons are independent, a conjunction analysis was performed in SPM2 to identify auditory brain areas that were typically responsive to both IRNs (Nichols et al., 2005). The conjunction of the two contrasts revealed bilateral activity on the posterior edge of HG (9 and 38 voxels on the left and right sides respectively). Because of the smaller dataset sizes, the results reached significance only at the uncorrected level ($P < 0.001$). The peaks of activity most likely corresponded to the primary field Te1.0; with a 30% probability on the left (-54, -20, 8 mm) and a 70% probability on the right (54, -16, 6 mm). Common pitch-related activity was again predominantly encompassed within the low-FDRR (Figure 2D). In summary, these data support the claim that the pitch-related response is somewhat constant across two pitch evoking stimuli that differ spectrally. While this is consistent with the notion of a pitch map, our evidence is not definitive since one would also be required to demonstrate an orderly progression of response preferences across a range of fundamental frequencies.

Individual listeners

The combined group results generally support both main hypotheses; sensitivities to periodicity and low-frequency were typically co-localised and this region encompassed primary auditory cortex in the lateral part of HG, as well as adjacent nonprimary regions. Unfortunately in fMRI, the degree of spatial precision in identifying patterns of functional activity is somewhat obscured by the data averaging procedure necessary for the group analysis. In addition, residual anatomical variability in the arrangement of the auditory fields across brains is without question (Morosan et al., 2001; Rademacher et al., 2001) and individual variability in the distribution of functional activation is observed both for frequency (Formisano et al., 2003; Talavage et al., 2000; 2004) and pitch (Patterson et al., 2002; Penagos et al., 2004). To circumvent these problems, we reanalysed the data using individual analyses based on image data that were more lightly spatially smoothed (3.25 mm^3 , full width half maximum) with minimal compromise of the original spatial resolution. **In contrast to the group data, which failed to reveal any high-frequency activation in the left auditory cortex, we found individuals whom clearly showed significant high-frequency responses around HG. For example, Figure 3 illustrates a high-FDRR in left medial HG on slice 2 for listener (iv), on slice 3 for listener (xii) and on slice 2 listener (xiii).** In this section, we report how the overlap between frequency and pitch-related activation varied from listener to listener.

**** Figure 3 ****

For each listener, we determined the number of voxels that were sensitive to both periodicity and low- and high-frequency respectively. Once again, the FDRRs were defined by contrasts for the tone and noise conditions combined and we report the results at two different probability thresholds within the ROI; i) $p < 0.001$ uncorrected and, ii) $p < 0.05$ corrected for a false-discovery rate. Counts of the number of activated voxels are reported in Table 2. Unlike the group results, the individual data revealed that, in some listeners, both left and right auditory cortices were

responsive to high-frequency stimuli and moreover that parts of the high-FDRR were also sensitive to temporal pitch. **These effects had been obscured by the combined group results.** Nevertheless, the individual results again demonstrated significantly greater overlap in the low-FDRR than in the high-FDRR. When the results reported at the uncorrected threshold are expressed as a mean percentage, 47% (124/265 voxels) of the total periodicity-related activation occurred in the low-FDRR, while a mere 1% (3/265) occurred in the high-FDRR. **Even individuals who produced reasonably large clusters of high-frequency activation around HG showed little or no evidence that this overlapped with the pitch response.** For example, taking the three listeners (iv, xii and xiii) described previously who had 59, 130 and 39 voxels of significant high-frequency activation in the left auditory ROI, only 1 of these voxels, for listener (xii), was co-activated by pitch. A Mantel-Haenszel test of conditional independence was carried out on the 2x2 contingency tables (periodicity/no periodicity x low-FDRR/high-FDRR) stratified by listener. This test confirmed that the proportion of the periodicity-related response occurring within the low-FDRR was reliably greater than that in the high-FDRR ($\chi^2 = 124.2$ in the left hemisphere and $\chi^2 = 270.9$ in the right hemisphere, $p < 0.001$). **Note that the analysis was performed on the proportions of co-activity and so does not bias against the smaller sizes of the high-FDRR.** The same pattern was maintained for the results reported at the corrected statistical threshold, but this more stringent procedure lead to a greater number of zero cases.

In summary, the individual results again support the view that frequency and periodicity coding have a common neural substrate in the human auditory cortex, and this is typically shifted towards the low-frequency-sensitive region.

** Table 2 **

Experiment 2 :

A reasonable rationale for using IRN stimuli to examine pitch coding in the central auditory system was that it built on a large body of existing evidence on temporal pitch in humans using both

fMRI and MEG. Our choice of stimulus parameters for creating the IRN was therefore influenced by those previous experiments. Unfortunately, none of these studies adequately rule out the contribution of neural responses to low-frequency distortions for spectrally-complex stimuli. Although the IRN input contains no spectral information at the frequency at which the pitch is heard, when those IRNs are presented at the high sound levels required for fMRI, additional combination tones are generated by the nonlinear mechanics of the cochlea. The combination tones include a peak at the frequency of the pitch and peaks of decreasing energy across the higher harmonics. There are large individual differences in the audibility of combination tones but, on average, the fundamental component becomes detectable when the complex tone reaches a presentation level of about 67 dB SPL (Plomp, 1965). This phenomenon is a major confounding issue in many studies of periodicity coding and the presence of significant distortion has recently been demonstrated in the neural representation of pitch in the inferior colliculus (McAlpine, 2004). As a consequence, the simplest explanation of the results reported in Experiment 1 is that the low-frequency area merely responded to the distortion produced by the high-pass filtered IRNs that corresponded to the fundamental frequency. In Experiment 2, we controlled for the effects of distortion in temporal pitch coding by adding a low-frequency masker noise to the stimuli.

Four of the original listeners returned to participate in Experiment 2 (listeners i, xi, xiii and xiv). All of these listeners had produced the typical pattern of periodicity- and frequency-related responses reported in Experiment 1. Stimulus parameters, protocol for the fMRI experiment and image analyses were the same as those described in Experiment 1; the only difference being that all the stimuli were resynthesised with the addition of a low-frequency noise masker. The masker contained frequencies between 25 and 150 Hz to encompass both the fundamental frequency and the second harmonic component of the pitch-evoking IRNs. The average energy across frequencies in the passband of the masker was matched to the energy of the components in the IRN (-39 dB relative to the maximum scale). Psychophysical (Pressnitzer et al., 2001) and physiological

(McAlpine, 2004) evidence indicate that this masker level is sufficient to exceed the level of the distortions.

** Table 3 **

Results

We report the results for individual listeners because there was insufficient power to combine the data in a group analysis (Table 3). Although the mean response was predominantly driven by one listener (xiv), at least a small amount of significant periodicity-related activity was observed in all four listeners. Thus, the addition of masker noise to remove the contribution from any neural energy at the fundamental frequency of the pitch did *not* eliminate the IRN effect. In line with the results from Experiment 1, periodicity coding generally engaged parts of lateral HG and anterolateral PT. For example, the peaks of the periodicity response for listener (xiv) were at the coordinates -50, -8, 2 mm and 64, -12, 4 mm. Although the amount of periodicity-related activation varied from listener to listener, it was again more likely to overlap with the low- than the high-FDRR. When the voxel counts reported at the uncorrected threshold ($p < 0.001$) are expressed as a mean percentage, 40% (86/215 voxels) of the total pitch-related activation occurred in the low-FDRR, while a mere 1% (3/215) occurred in the high-FDRR. These results rule out the explanation that the low-frequency area simply responds to the spectral distortion produced by IRN stimuli.

Discussion

Our results in human auditory cortex are entirely consistent with the neurophysiological evidence for a role in coding both frequency and pitch properties of sound. Our experiment revealed a good correspondence between sensitivity to low-frequency and periodic structure that included the two lateralmost primary fields (Te1.0 and Te1.2) and extended posteriorly across part of PT. This

pattern of activation was repeatedly identified for a majority of listeners and had a fairly consistent position relative to anatomical landmarks. Pitch-selectivity was established by the general response to temporal pitch, which was constant across two different frequency carriers, and by ruling out peripheral explanations in terms of spectral distortion. We therefore propose that this result represents a signature pattern of cortical periodicity and frequency sensitivity. Our findings are important because they corroborate a homology across human and non-human primate species for a pitch processing centre at the lateral boundary of the primary area, yet they are also intriguing because they direct neurophysiologists to explore pitch sensitivity in surrounding auditory fields.

How confident are we that both IRNs generate a pitch percept? Oxenham et al. (2004) recently demonstrated that the location along the tonotopic axis of the temporal acoustic information can severely impact on the perceived pitch. Transposing low-frequency temporal fine-structure information to locations in the cochlea tuned to high frequencies impaired pitch perception for single and harmonic-complex tones; a result that supports the important contribution of place representations for pitch coding. **Although we did not quantify the salience of the pitch evoked by the two IRN stimuli for the present set of listeners, previous measurements of pitch discrimination have been reported for IRN generated using comparable stimulus parameters. Discrimination performance provides a marker for the salience of a pitch-evoking stimulus. For example, Yost et al. (1998) examined pitch discrimination across a range of bandpass filter conditions for two IRN stimuli both with a delay of 16 ms and 8 iterations. One IRN stimulus had a gain of +1 (giving a pitch of $1/\text{delay}$), while the other had a gain of -1 (giving a pitch of $1/(2 \times \text{delay})$). For the low-spectrum IRNs (0.1-2.1 kHz passband), listeners were able to discriminate the two stimuli perfectly. Although discriminability did decline for the high-spectrum IRN (4-6 kHz passband), listeners still performed with 70% accuracy. Moreover, listeners were easily able to discriminate between the high-spectrum IRN and a matched noise (90% accuracy). Given the upper cutoff for the IRN presented in the current set of experiments fell below 6 kHz, these results indicate that both of our IRN stimuli convey**

temporal pitch information by their waveform fine structure. Thus the differences in pitch-related activation between the low-spectrum and the high-spectrum contrasts are unlikely to be due to any inability to hear a pitch in the high-spectrum IRN.

Interpreting the fMRI results with respect to probabilistic anatomy suggested that the response to periodicity engaged primary, as well as nonprimary, auditory cortical regions. This result calls for further scrutiny, not least because Schwarz and Tomlinson (1990) failed to record any pitch-related response in primary auditory neurons of the alert monkey. The precise homologies between different species are difficult to establish, but on the basis of anatomy (i.e. cytoarchitectonic and histochemical staining and neural connectivity patterns) there is support for the primary (core) area in primates to be equivalent to the medial two-thirds of HG in humans (Hackett et al., 2001). In general, we observed periodicity-related responses to extend across the lateral two-thirds of HG (areas Te1.0 and Te1.2). Although the parcellation scheme given by Morosan et al. (2001) denotes Te1.2 (the lateral-third of HG) as belonging to the primary auditory cortex, it shares some histological properties with surrounding nonprimary fields (see also Wallace et al., 2002). Its transitional qualities therefore make Te1.2 a good candidate for correspondence with the anterolateral border of the primate core (Hackett et al., 2001). Thus, any apparent discrepancies between interpretations of the primate and the human data are most likely due differences in nomenclature than in functional organisation. Commonalities in the profile of the pitch-related response support this view. For example, in primates many neurons at the anterolateral border of the core exhibited increased discharge rate for pure tones presented at best-frequency and missing fundamental harmonic-complex tones with similar pitches, even when all the harmonic components were outside the neuron's excitatory frequency response area (Bendor and Wang, 2005). In addition, most of these pitch-selective neurons had best-frequencies below 400 Hz. The similarities with our fMRI data are persuasive. For example, the high-spectrum IRN contained frequencies above 3 kHz and yet this pitch-evoking stimulus produced a strong response in the same voxels that had a preference for low-frequency sounds.

To what extent this pitch area represents or unifies both spectral and temporal pitch processing strategies has yet to be resolved. Nevertheless, a body of human imaging research demonstrates a consistent involvement of lateral parts of the auditory cortex around HG in coding a wide range of pitch-evoking stimuli containing spectral components that are either resolved or unresolved by the auditory system. The technique of fMRI has been most successful in defining the region of the human auditory cortex that is sensitive to pitch processing. These results have demonstrated a restricted region within lateral HG that is sensitive to harmonic-complex tones containing resolved and/or unresolved harmonics (Penagos et al., 2004). Source estimates for magnetoencephalography (MEG) data are consistent with this auditory region being responsible for the analysis of other pitch-evoking stimuli including click trains (Gutschalk et al., 2002), tones in noise and Huggins pitch (Chait et al., 2006). By far the most commonly used pitch-evoking stimulus is the temporal pitch, IRN. Again, lateral HG appears to be strongly responsive to an IRN relative to a spectrally-matched noise; measured using fMRI (Barrett and Hall, 2006; Griffiths et al., 1998; Hall et al., 2005; Patterson et al., 2002) and MEG (Krumbholz et al., 2003; Ritter et al., 2005).

Several workers have used MEG to map the axis of pitch coding and to define its spatial correspondence to the underlying tonotopic organisation in the same listeners. Langner et al. (1997) have argued for two linear tonotopic and periodicity gradients across human auditory cortex oriented at approximately 90° to one another. This interpretation remains controversial; first, because frequency sensitivity was mapped using single sinusoids which do not separate frequency from periodicity representations and second, because the conclusion assumes that the mean orientation is the most representative summary of the individual results (Lütkenhöner, 2003). Subsequent MEG studies have addressed the first criticism by independently manipulating frequency and periodicity using harmonic-complex tones, but have failed to replicate this orthogonality. Instead, the results appear to reveal that the spatial representation of spectral content dominates over periodicity pitch (Cansino et al., 2003; Crottaz-Herbette and Ragot, 2000). While

the frequency gradients plotted for sinusoids and periodic complex tones differed in these studies, the authors conclude that frequency and pitch representations overlap one another in a non-independent manner.

For Peer Review

Acknowledgements

Scanning was supported by the Department of Communication Sciences and Disorders, University of South Carolina. We thank Professor Gordon Baylis and Dr Paul Morgan who facilitated this project. We also thank Deafness Research (UK) who funded Ms Rosalind Holmes as a vacation scholar to work on some of the initial analysis.

For Peer Review

References

- Barrett, D. J. K. & Hall, D. A. (2006) Response preferences for 'what' and 'where' in human non-primary auditory cortex. *NeuroImage*, **32**, 968-977.
- Bendor, D. & Wang, X. (2005) The neuronal representation of pitch in primate auditory cortex. *Nature* **436**, 1161-1165.
- Cansino, S., Ducorps, A. & Ragot, R. (2003) Tonotopic cortical representation of periodic complex sounds. *Hum. Br Mapp* ., **20**, 71-81.
- Chait, M., Poeppel, D. & Simon, J.Z. (2006) Neural correlates of detection of monaurally and binaurally created pitches in humans. *Cereb. Cort.*, **16**, 835-848.
- Crottaz-Herbette, S. & Ragot R. (2000) Perception of complex sounds: N1 latency codes pitch and topography codes spectra. *Clin. Neurophysiol.*, **111**, 1759-1766.
- Eickhoff, S. B., Stephan, K. E., Mohlberg, H., Grefkes, C., Fink, G. R., Amunts, K. & Zilles, K. (2005) A new SPM toolbox for combining probabilistic cytoarchitectonic maps and functional imaging data. *NeuroImage*, **25**, 1325-1335.
- Formisano, E., Kim, D-S., Di Salle, F., van de Moortele, P-F., Urgibil, K. & Goebel, R. (2003) Mirror-symmetric tonotopic maps in human primary auditory cortex. *Neuron*, **40**, 859-869.
- Griffiths, T. D., Buchel, C., Frackowiak, R. S. & Patterson, R. D. (1998) Analysis of temporal structure in sound by the human brain. *Nat. Neurosci.*, **1**, 422-427.
- Gutschalk, A., Patterson, R. D, Rupp, A., Uppenkamp, S. & Scherg, M. (2002) Sustained magnetic fields reveal separate sites for sound level and temporal regularity in human auditory cortex. *NeuroImage*, **15**, 207–216.
- Hackett, T. A., Preuss, T. M. & Kaas, J.H. (2001) Architectonic identification of the core region in auditory cortex of macaques, chimpanzees and humans. *J. Comp. Neurol.*, **441**, 197-222.
- Hall, D. A., Haggard, M. P., Akeroyd, M. A., Palmer, A. R., Summerfield, A. Q., Elliott, M. R., Gurney, E. & Bowtell, R. W. (1999) Sparse temporal sampling in auditory fMRI. *Hum. Br. Mapp.*, **7**, 213-223.

- Hall, D. A., Barrett, D. J. K., Akeroyd, M. A. & Summerfield, A. Q. (2005) Cortical representations of temporal structure in sound. *J. Neurophysiol.*, **94**: 3181–3191.
- Harms, M. P., & Melcher, J. R. (2002) Sound repetition rate in the human auditory pathway: Representations in the waveshape and amplitude of fMRI activation. *J. Neurophysiol.*, **88**: 1433–1450.**
- Krumbholz, K., Patterson, R. D., Seither-Preisler, A., Lammertmann, C. & Lütkenhöner, B. (2003) Neuromagnetic evidence for a pitch processing center in Heschl's gyrus. *Cereb. Cort.*, **13**, 765-772.
- Langner, G., Sams, M., Heil, P. & Schulze H. (1997) Frequency and periodicity are represented in orthogonal maps in the human auditory cortex: Evidence from magnetoencephalography. *J. Comp. Physiol. A*, **181**, 665-676.
- Lütkenhöner B. (2003) Single-dipole analyses of the N100m are not suitable for characterising the cortical representation of pitch. *Audiol. Neuroto l.*, **8**, 222-233.
- McAlpine, D. (2004) Neural sensitivity to periodicity in the inferior colliculus: Evidence for the role of cochlear distortions. *J. Neurophysiol.*, **92**, 1295-1311.
- Morosan, P., Rademacher, J., Schleicher, A., Amunts, K., Schormann, T. & Zilles. K. (2001) Human primary auditory cortex: Cytoarchitectonic subdivisions and mapping into a spatial reference system. *NeuroImage*, **13**, 684-701.
- Nichols, .T, Brett, M., Andersson, J., Wager, T. & Poline, J-B. (2005) Valid conjunction inference with the minimum statistic. *NeuroImage*, **25**, 653– 660.
- Oxenham, A. J., Bernstein, J. G. W. & Penagos, H. (2004) Correct tonotopic representation is necessary for complex pitch perception. *Proc. Nat. Acad. Sci.*, **101**, 1421–1425.
- Pantev, C., Hoke, M., Lehnertz, K., Lütkenhöner, B., Anogianakis, G. & Wittkowski, W. (1998) Tonotopic organization of the human auditory cortex revealed by transient auditory evoked magnetic fields. *Electroenceph. Clin. Neurophysiol.*, **69**: 160-170.
- Patterson, R. D., Handel, S., Yost, W. A. & Datta. J. (1996) The relative strength of the tone and noise components in iterated rippled noise. *J. Acoust. Soc. Am.*, **100**, 3286-3294.

- Patterson, R. D., Uppenkamp, S., Johnsrude, I. S. & Griffiths, T. D. (2002) The processing of temporal pitch and melody information in auditory cortex. *Neuron*, **36**, 767-776.
- Penagos, H., Melcher, J. R. & Oxenham, A. J. (2004) A neural representation of pitch salience in nonprimary human auditory cortex revealed with functional magnetic resonance imaging. *J. Neurosci.*, **24**: 6810-6815.
- Plomp R. (1965) Detectability threshold for combination tones. *J. Acoust. Soc. Am.*, **37**, 1110-1123..
- Pressnitzer, D. & Patterson, R. D. (2001) Distortion products and the perceived pitch of harmonic complex tones. In Breebart, D. J., Houtsma, A. J. M., Kohlrausch, A., Prijs, V. F. & Schoonoven, R. (eds), *Physiological and Psychophysical Bases of Auditory Function*. Shaker, Maastricht, pp. 97-104.
- Rademacher, J., Morosan, P., Schormann, T., Schleicher, A., Werner, C., Freund, H-J. & Zilles K. (2001) Probabilistic mapping and volume measurement of human primary auditory cortex. *NeuroImage*, **13**, 669-683.
- Ritter, S., Dosch, H. G., Specht, H-J. and Rupp, A. (2005) Neuromagnetic responses reflect the temporal pitch change of regular interval sounds. *NeuroImage*, **27**, 533-543.
- Romani, G. L., Williamson, S. J., Kaufman, L. (1982) Tonotopic organization of the human auditory cortex. *Science*, **216**: 1339-1340.
- Schulze, H. & Langner, G. (1997) Periodicity coding in the primary auditory cortex of the Mongolian gerbil (*Meriones unguiculatus*): Two different coding strategies for pitch and rhythm? *J. Comp. Physiol. A*, **181**, 651-663.
- Schulze, H., Hess, A., Ohl, F. W. & Scheich, H. (2002) Superposition of horseshoe-like periodicity and linear tonotopic maps in auditory cortex of the Mongolian gerbil. *Eur. J. Neurosci.*, **15**, 1077-1084.
- Schwarz, D. W. F. & Tomlinson, R. W. W. (1990) Spectral response patterns of auditory-cortex neurons to harmonic complex tones in alert monkey (*Macaca mulatta*). *J. Neurophysiol.*, **64**, 282-298.

- Talavage, T. M., Ledden, P. J., Benson, R. R., Rosen, B. R. & Melcher, J. R. (2000) Frequency-dependent responses exhibited by multiple regions in human auditory cortex. *Hear. Res.*, **150**, 225-244.
- Talavage, T. M., Sereno, M. I., Melcher, J. R., Ledden, P. J., Rosen, B. R. & Dale, A. M. (2004) Tonotopic organization in human auditory cortex revealed by progressions of frequency sensitivity. *J. Neurophysiol.*, **91**, 1282-1296.
- Yost, W. A., Patterson, R. D. & Sheft, S. (1996) A time-domain description for the pitch strength of iterated rippled noise. *J. Acoust. Soc. Am.*, **99**, 1066–1078.
- Yost W. A., Patterson, R. & Sheft, S. (1998) The role of the envelope in processing iterated rippled noise. *J. Acoust. Soc. Am.*, **104**, 2349-2361.
- Wallace, M. N., Johnston, P. W. & Palmer, A. R. (2002) Histochemical identification of cortical areas in the auditory region of the human brain. *Exp. BrRes.*, **143**, 499-508.
- Wessinger, C. M., VanMeter, J., Tian, B., Van Lare, J., Pekar, J. & Rauschecker, J.P. (2001) Hierarchical organisation of the human auditory cortex revealed by functional magnetic resonance imaging. *J. Cog. Neurosci.*, **13**, 1-7.
- Westbury, C. F., Zatorre, R. J. & Evans, A. C. (1999) Quantifying variability in the planum temporale: A probability map. *Cereb. Cort.*, **9**, 392-405.

Table legends

Table 1. The location and extent of frequency- and periodicity-related activation resulting from the group-averaged analyses. Co-ordinates and Z values are reported for the peaks of maximum significance within each cluster. We report two values for the cluster size; the first value relates to a $p < 0.001$ threshold uncorrected for multiple comparisons and the value in parentheses relates to a $p < 0.05$ threshold, controlled for a false discovery rate. Except for the high-FDRR, peaks are significant at both statistical thresholds. Confidence ratings for the localization of these peaks are taken from the probability values corresponding to those co-ordinates reported for subdivisions of HG using the SPM anatomy toolbox (Eickhoff et al., 2005) and of PT using the values given by Westbury et al. (1999).

Table 2. Individual patterns of periodicity- and frequency-related activation, and their intersections, from Experiment 1. The number of suprathreshold voxels within the ROI are reported separately for the left and right auditory cortex and for the same two probability thresholds that are described in Table 1.

Table 3. Individual patterns of periodicity- and frequency-related activation, and their intersections, in Experiment 2. As in Table 2, the number of suprathreshold voxels within the ROI are reported separately for the left and right auditory cortex and for two probability thresholds.

Figure legends

Figure 1. Simulated neural excitation patterns to pure tone, random noise and iterated-ripple-noise (IRN) stimuli at centre frequencies of 800 Hz (first column) and 4500 Hz (second column). Fifteen examples of the noise stimuli are plotted in panels C-F to illustrate the lack of structure in the excitation pattern. The abscissa is scaled according to the tonotopic dimension of hearing and represents the place of excitation along the basilar membrane. An ERB refers the equivalent

rectangular bandwidth of the auditory filter with each ERB corresponding to a distance of about 0.89 mm on the basilar membrane. Stimuli were carefully constructed to excite the same number of ERB filters and hence the same sized distance along the basilar membrane. The IRN was constructed by delaying a copy of a random noise by 16.67 ms (1/60 Hz), adding it back to the original noise and repeating this process 16 times to introduce temporal regularity (Yost et al., 1996; see Materials and Methods for details).

Figure 2. Various illustrations of the distribution of frequency- and periodicity-related activations ($p < 0.001$ uncorrected) from Experiment 1. (A) illustrates the FDRRs for the tone and noise conditions combined into a single statistical contrast. (B) and (C) illustrate the separate contribution of the tone and the noise conditions to each of the FDRRs. Finally, (D) presents the location of the pitch-constant response; significant in both low- and high-spectrum IRN conditions. The four slices span the auditory cortex in both hemispheres, displayed on the mean anatomical scan with the left hemisphere on the left hand side. Slices are oriented parallel to the Sylvian fissure with the first slice taken along the top of the supratemporal plane. Successive slices are taken 4mm apart with the fourth slice close to the boundary of the superior temporal sulcus, as shown on the sagittal view.

Figure 3. Individual results for each of the 14 listeners. Activations for the three main frequency- and periodicity-related activations are shown using the same colour scheme and slice orientation as in Figure 2. Here, activations are overlaid onto the individual's own anatomical scan, thus preserving any residual variability in gyral patterning. The white region denotes the probabilistic location of lateral HG (Te1.2) given by Morosan et al. (2001).

Peak MNI coordinate mm			Cluster size # voxels	Z value	Side	Putative anatomical region	Localization confidence
x	y	z					
Low-FDRR							
-48	-22	6	428 (995)	4.91	L	Central HG	80.0
-52	-12	6	“	4.66	“	Lateral HG	40.0
-64	-16	0	“	4.50	“	Anterolateral PT	21.6
58	-6	-2	431 (745)	4.95	R	Lateral HG	50.0
68	-24	0	“	4.56	“	Lateral PT	13.5
66	-16	2	“	4.09	“	Lateral PT	24.4
High-FDRR							
44	-16	0	12 (n.s)	3.77	R	Central HG	30.0
40	-26	4	12 (n.s)	3.74	R	Medial HG	70.0
54	-30	14	39 (n.s)	3.67	R	Central PT	67.4
Periodicity-sensitive region							
-66	-20	16	77 (282)	3.96	L	Anterior lateral PT	10.9
-50	-26	8	“	3.50	“	Anterior central PT	81.1
-60	-14	-2	“	3.41	“	Inferior lateral PT	8.1
52	-18	6	220 (493)	4.02	R	Central HG	80.0
66	-14	-4	“	3.86	“	Inferior lateral PT	5.4
70	-24	-2	“	3.82	“	Inferior lateral PT	5.4

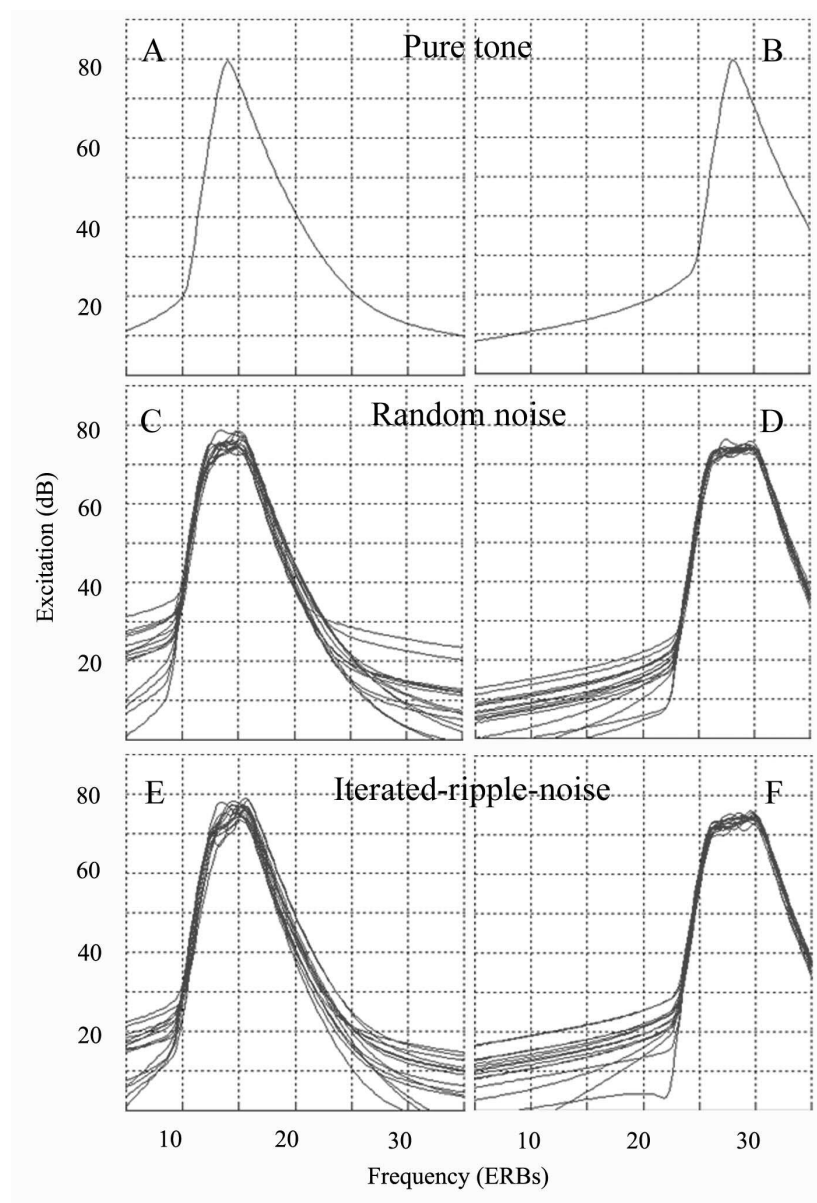
Table 1. The location and extent of frequency- and periodicity-related activation resulting from the group-averaged analyses. Co-ordinates and Z values are reported for the peaks of maximum significance within each cluster. We report two values for the cluster size; the first value relates to a $p < 0.001$ threshold uncorrected for multiple comparisons and the value in parentheses relates to a $p < 0.05$ threshold, controlled for a false discovery rate. All peaks are significant at both statistical thresholds. Confidence ratings for the localization of these peaks are taken from the probability values corresponding to those co-ordinates reported for subdivisions of HG using the SPM anatomy toolbox (Eickhoff et al., 2005) and of PT using the values given by Westbury et al. (1999).

Subject	Total pitch-sensitive		Pitch sensitive in low-FDRR		Pitch sensitive in high-FDRR		Total low-FDRR		Total high-FDRR	
	L	R	L	R	L	R	L	R	L	R
<i>Uncorrected</i>										
i	94	49	59	24	0	1	290	233	11	78
ii	329	148	142	98	0	0	417	323	1	106
iii	0	31	0	17	0	0	427	383	100	65
iv	2	0	0	0	0	0	405	304	59	128
v	114	189	53	66	0	0	173	110	31	12
vi	70	85	63	76	0	0	296	260	40	53
vii	130	102	99	86	0	0	279	311	90	174
viii	4	0	0	0	0	0	332	265	140	128
ix	447	271	152	75	13	30	441	241	55	199
x	2	0	0	0	0	0	143	38	13	76
xi	214	198	115	165	4	0	791	526	9	28
xii	288	194	131	117	1	0	307	369	130	82
xiii	60	150	2	21	0	0	144	66	39	275
xiv	361	183	66	114	0	2	317	279	16	63
<i>Mean</i>	<i>151</i>	<i>114</i>	<i>63</i>	<i>61</i>	<i>1</i>	<i>2</i>	<i>340</i>	<i>265</i>	<i>52</i>	<i>105</i>
<i>Corrected using a false discovery rate method</i>										
i	1	0	1	0	0	0	207	177	0	9
ii	178	88	68	56	0	0	305	239	0	50
iii	0	0	0	0	0	0	277	296	36	8
iv	0	0	0	0	0	0	296	221	14	75
v	10	79	3	29	0	0	72	52	0	0
vi	0	1	0	1	0	0	216	198	12	3
vii	42	38	40	37	0	0	198	230	8	90
viii	0	0	0	0	0	0	238	213	65	30
ix	262	118	55	32	6	8	339	185	24	129
x	0	0	0	0	0	0	56	4	1	38
xi	90	110	35	87	0	0	653	462	0	0
xii	257	175	85	68	0	0	164	200	43	39
xiii	6	73	0	3	0	0	54	21	8	130
xiv	276	135	38	89	0	0	175	219	4	20
<i>Mean</i>	<i>80</i>	<i>58</i>	<i>23</i>	<i>29</i>	<i>0</i>	<i>1</i>	<i>232</i>	<i>194</i>	<i>15</i>	<i>44</i>

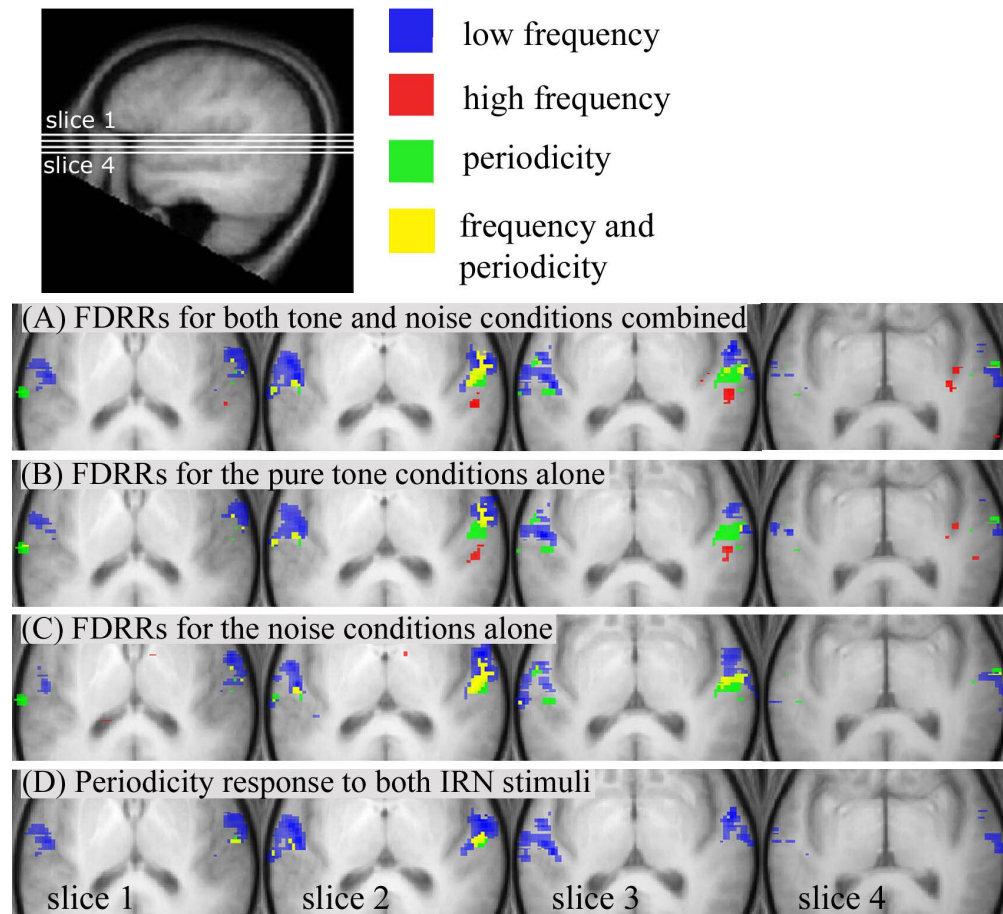
Table 2. Individual patterns of periodicity- and frequency-related activation, and their intersections, from Experiment 1. The number of suprathreshold voxels within the ROI are reported separately for the left and right auditory cortex and for the same two probability thresholds that are described in Table 1.

Subject	Total pitch-sensitive		Pitch sensitive in low-FDRR		Pitch sensitive in high-FDRR		Total low-FDRR		Total high-FDRR	
	L	R	L	R	L	R	L	R	L	R
<i>Uncorrected</i>										
i	8	25	0	0	0	0	240	226	0	0
xi	10	0	2	0	0	0	319	361	8	147
xiii	1	0	1	0	0	0	465	410	57	140
xiv	594	146	218	123	6	5	621	678	218	283
<i>Mean</i>	<i>153</i>	<i>62</i>	<i>55</i>	<i>31</i>	<i>2</i>	<i>1</i>	<i>411</i>	<i>419</i>	<i>71</i>	<i>106</i>
<i>Corrected using a false discovery rate method</i>										
i	0	0	0	0	0	0	98	97	0	0
xi	0	0	0	0	0	0	203	276	0	38
xiii	0	0	0	0	0	0	354	325	17	56
xiv	419	84	170	81	1	1	556	628	185	135
<i>Mean</i>	<i>105</i>	<i>21</i>	<i>43</i>	<i>20</i>	<i>0</i>	<i>0</i>	<i>232</i>	<i>332</i>	<i>51</i>	<i>57</i>

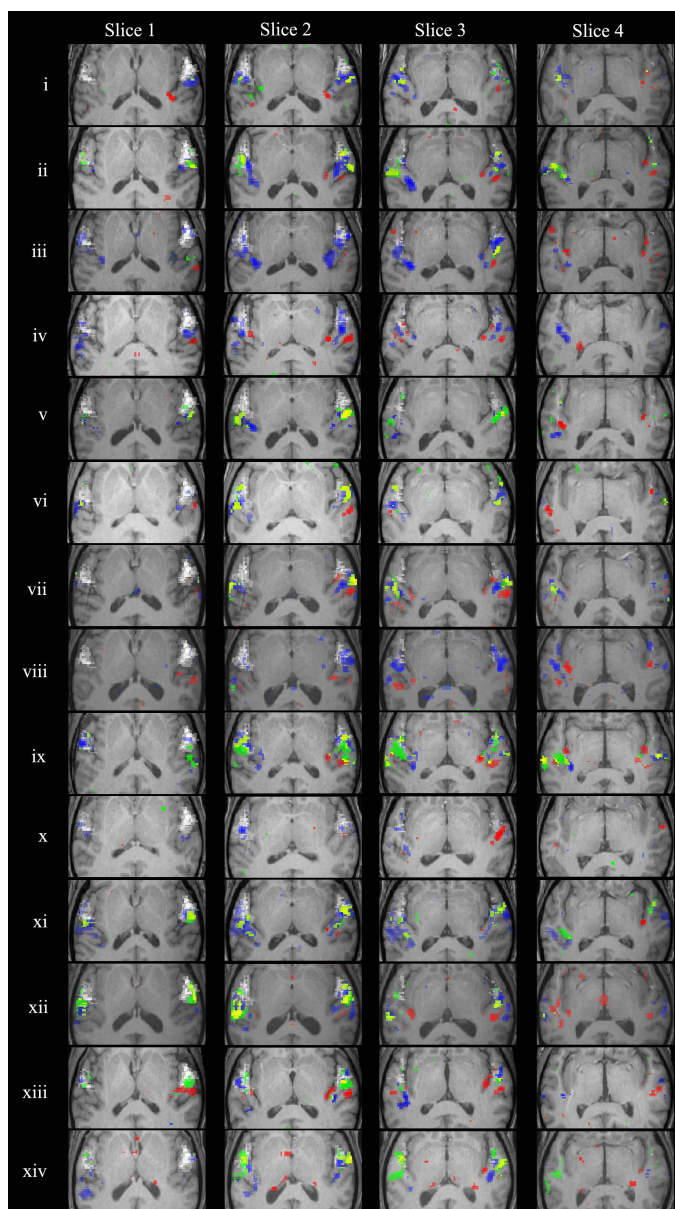
Table 3. Individual patterns of periodicity- and frequency-related activation, and their intersections, in Experiment 2. As in Table 2, the number of suprathreshold voxels within the ROI are reported separately for the left and right auditory cortex and for two probability thresholds.



Simulated neural excitation patterns to pure tone, random noise and iterated-ripple-noise (IRN) stimuli at centre frequencies of 800 Hz (first column) and 4500 Hz (second column). Fifteen examples of the noise stimuli are plotted in panels C-F to illustrate the lack of structure in the excitation pattern. The abscissa is scaled according to the tonotopic dimension of hearing and represents the place of excitation along the basilar membrane. An ERB refers the equivalent rectangular bandwidth of the auditory filter with each ERB corresponding to a distance of about 0.89 mm on the basilar membrane. Stimuli were carefully constructed to excite the same number of ERB filters and hence the same sized distance along the basilar membrane. The IRN was constructed by delaying a copy of a random noise by 16.67 ms (1/60 Hz), adding it back to the original noise and repeating this process 16 times to introduce temporal regularity (Yost et al., 1996; see Materials and Methods for details).



Various illustrations of the distribution of frequency- and periodicity-related activations ($p < 0.001$ uncorrected) from Experiment 1. (A) illustrates the FDRRs for the tone and noise conditions combined into a single statistical contrast. (B) and (C) illustrate the separate contribution of the tone and the noise conditions to each of the FDRRs. Finally, (D) presents the location of the pitch-constant response; significant in both low- and high-spectrum IRN conditions. The four slices span the auditory cortex in both hemispheres, displayed on the mean anatomical scan with the left hemisphere on the left hand side. Slices are oriented parallel to the Sylvian fissure with the first slice taken along the top of the supratemporal plane. Successive slices are taken 4mm apart with the fourth slice close to the boundary of the superior temporal sulcus, as shown on the sagittal view.



Individual results for each of the 14 listeners. Activations for the three main frequency- and periodicity-related activations are shown using the same colour scheme and slice orientation as in Figure 2. Here, activations are overlaid onto the individual's own anatomical scan, thus preserving any residual variability in gyral patterning. The white region denotes the probabilistic location of lateral HG (Te1.2) given by Morosan et al. (2001).